Effects of Degassing on the Long-Range Attractive Force between Hydrophobic Surfaces in Water

Hallam Stevens,[§] Robert F. Considine,[||] Calum J. Drummond,*[,†] Robert A. Hayes,[⊥] and Phil Attard*[,‡]

CSIRO Molecular Science, P.O. Box 184, North Ryde New South Wales 1670, Australia, School of Chemistry F11, University of Sydney, New South Wales 2006, Australia, Department of the History of Science, Harvard University, Science Center 371, Cambridge, Massachusetts 02138, Barwon Water, Post Office Box 659, Geelong Victoria 3220, Australia, and Philips Research Laboratories, Professor Holstlaan 4 (WY72) 5656 AA Eindhoven, The Netherlands

Received March 21, 2005. In Final Form: April 20, 2005

The long-ranged attractions between hydrophobic amorphous fluoropolymer surfaces are measured in water with and without dissolved air. An atomic force microscope is used to obtain more than 500 measured jump-in distances, which yields statistically reliable results. It is found that the range of the attraction and its variability is generally significantly decreased in deaerated water as compared to normal, aerated water. However, the range and strength of the attraction in deaerated water remain significantly greater than the van der Waals attraction for this system. The experimental observations are consistent with (1) nanobubbles being primarily responsible for the long-ranged attraction in normal water, (2) nanobubbles not being present in deaerated water when the surfaces are not in contact, and (3) the attraction in the absence of nanobubbles being most probably due to the approach to the separation-induced spinodal cavitation of the type identified by Bérard et al. [*J. Chem. Phys.* **1993**, *98*, 7236]. It is argued that the measurements in deaerated water reveal the bare or pristine hydrophobic attraction unobscured by nanobubbles.

Introduction

The hydrophobic interaction is the primary mechanism involved in the folding of polypeptide chains into protein structures; it determines the structure and morphology of many block copolymers, and it controls the self-assembly of amphiphilic molecules. Moreover, hydrophobic effects are crucial in the development of ultralow surface free energy materials and nonwetting surfaces, in controlling the stability of colloidal dispersions, and in separating minerals by flotation. A number of reviews have appeared of direct force measurements between macroscopic hydrophobic surfaces in water.[1,2] Although the existence of a strong force of attraction between hydrophobic surfaces is not disputed, there exist significant discrepancies in the magnitude and range of the force as measured by different experimenters. This situation has meant that theories that attribute the hydrophobic force to water structure,[3] long-range electrostatic forces,[4,5] or induced cavitation[6−10] have thus far failed to convincingly account for all of the available experimental data.

A more promising explanation of the hydrophobic force, one that has gained significant experimental support over the past few years, asserts that submicroscopic bubbles (nanobubbles) adhering to the surfaces coalesce to form a bubble-bridge that draws the surfaces into contact.[11] The attractive force arises from the tension of the bridging bubble due to the unfavorable air−water interfacial energy, and this attraction increases as the bridging bubble spreads laterally along the surfaces.[12] The experimental evidence in favor of the bridging nanobubble mechanism includes the observation of steps or discontinuities in the force due to multiple bridging events,[11] the variability in the measured forces, which is taken to be due to variable bubble size,[11,13] and the observation of a short-range repulsion prior to the onset of the long-range attraction, which has been taken to be an electric double layer repulsion due to the charged bubble surface.[13−16] The measurement of qualitatively similar long-ranged attractions in other solvents between solvophobic walls has likewise been taken as evidence for nanobubbles and against water structure or electrostatic effects.[17] In addition, nanobubbles on hydrophobic surfaces have been imaged using atomic force microscopy.[15,16,18,19] There is

* Corresponding authors. E-mail: calum.drummond@csiro.au (C.J.D.); attard@chem.usyd.edu.au (P.A.).
† CSIRO Molecular Science.
‡ University of Sydney.
§ Harvard University.
|| Barwon Water.
⊥ Philips Research Laboratories.

(1) Christenson, H. K.; Claesson, P. M. *Adv. Colloid Interface Sci.* **2001**, *91*, 391.
(2) Attard, P. *Adv. Colloid Interface Sci.* **2003**, *104*, 75.
(3) Eriksson, J. C.; Ljunggren, S.; Claesson, P. M. *J. Chem. Soc., Faraday Trans. 2* **1989**, *85*, 163.
(4) Attard, P. *J. Phys. Chem.* **1989**, *93*, 6441.
(5) Podgornik, R. *J. Chem. Phys.* **1989**, *91*, 5840.
(6) Bérard, D. R.; Attard, P.; Patey, G. N. *J. Chem. Phys.* **1993**, *98*, 7236.
(7) Yaminsky, V. V.; Yushchenko, V. S.; Amelina, E. A.; Shchukin, E. D. *J. Colloid Interface Sci.* **1983**, *96*, 301.
(8) Yushchenko, V. S.; Yaminsky, V. V.; Shchukin, E. D. *J. Colloid Interface Sci.* **1983**, *96*, 307.
(9) Lum, K.; Chandler, D.; Weeks, J. D. *J. Phys. Chem. B* **1999**, *103*, 4570.
(10) Wennerström, H. *J. Phys. Chem. B* **2003**, *107*, 13772.
(11) Parker, J. L.; Claesson, P. M.; Attard, P. *J. Phys. Chem.* **1994**, *98*, 8468.
(12) Attard, P. *Langmuir* **1996**, *12*, 1693.
(13) Carambassis, A.; Jonker, L. C.; Attard, P.; Rutland, M. W. *Phys. Rev. Lett.* **1998**, *80*, 5357.
(14) Considine, R. F.; Hayes, R. A.; Horn, R. G. *Langmuir* **1999**, *15*, 1657.
(15) Tyrrell, J. W. G.; Attard, P. *Phys. Rev. Lett.* **2001**, *87*, 176104.
(16) Tyrrell, J. W. G.; Attard, P. *Langmuir* **2002**, *18*, 160.
(17) Considine, R. F.; Drummond, C. J. *Langmuir* **2000**, *16*, 631.
(18) Ishida, N.; Inoue, T.; Miyahara, M.; Higashitani, K. *Langmuir* **2000**, *16*, 6377.
(19) Lou, S.-T.; Ouyang, Z.-Q.; Zhang, Y.; Li, X.-J.; Hu, J.; Li, M.-Q.; Yang, F.-J. *J. Vac. Sci. Technol., B* **2000**, *18*, 2573.

10.1021/la0507535 CCC: $30.25
Published on Web 05/21/2005

also spectroscopic[20] and neutron reflectivity[21] evidence for gas films at hydrophobic surfaces.

In the bridging bubble theory for the long-ranged hydrophobic attraction, the range of the hydrophobic force is taken to be an indication of the height of the preexisting bubble on the isolated surface.[11] This leads to the prediction that the long-ranged hydrophobic attraction should disappear in deaerated water, assuming that deaeration completely removes the bubbles from the surfaces. If for some reason deaeration merely reduces the size or number of such bubbles, then one might expect it to reduce the hydrophobic attraction in range and possibly also in magnitude. In either case, determining whether the force between hydrophobic surfaces is sensitive to the amount of dissolved gas is essential in advancing the discussion over the nature of the long-range hydrophobic force.

The dependence of the hydrophobic interaction on the amount of dissolved gas has previously been explored in several laboratories. In some cases, large and systematic decreases in the range of the hydrophobic attraction upon deaeration have been reported.[14,22,23] In other cases, either no decrease in the attraction was reported,[24] or else the decrease was small but statistically significant.[25] In all cases, the attraction in deaerated water remained measurably more long ranged than the van der Waals attraction.[14,22−26] In the case of water saturated with argon, which is about twice as soluble as nitrogen, the attraction was reported to have increased.[27] In view of the other experimental evidence for the existence of nanobubbles on hydrophobic surfaces mentioned above, the inconclusive nature of the force measurements in deaerated systems is puzzling.

In this study, we carry out a systematic investigation into the effects of degassing on the long-range hydrophobic attraction. The surface used is an amorphous copolymer of perfluoro(2,2-dimethyl-1,3-dioxole) and tetrafluoroethylene (Teflon AF1600, where the ratio of dioxole to TFE is 66:34) with a surface free energy of 16.4 ± 1.4 mN m^{-1},[28] very close to the theoretical lower limit for a solid organic polymer. Advancing contact angles of water on Teflon AF1600 have been reported as 120°[17,28] and $121.5 \pm 1.4°$.[29] Receding contact angles of water on Teflon AF1600 have been reported as 109°[17] and $111.9 \pm 1.9°$.[29] We chose such a strongly hydrophobic surface to magnify the inherent hydrophobic attraction, and hence to observe unambiguously the effects of degassing. The cast fluoropolymer film has been shown to be smooth (0.3 nm root-mean-square roughness[28]), hard, amorphous (not crystalline or patchy), and devoid of loose condensates; as such, it is ideal for surface force measurement. The cast film is neutral and very stable, and so we avoid possible complications such as surfactant desorption, monolayer rearrangement, electrostatic interactions, or polymer mounds or trails, which have in some cases been argued to be present in other hydrophobic surface preparations, and which have created doubt, reasonable or otherwise, on the reported long-range attractions.

A further feature of the present investigation is the very large number of force measurements that we perform, which provides statistically reliable results. This was done with the usual repeated contact at a single point method, and also using the force−volume function of the atomic force microscope (AFM). This allows us to discuss the forces over a greatly extended contact region. The force map over such a region provides a useful point of comparison with data from repeated interactions at one contact site that potentially yields additional insight into the mechanism of the hydrophobic force.

We address the following questions: (1) Does deaeration significantly reduce the range of the hydrophobic attraction? (2) Is the magnitude and range of the hydrophobic attraction in deaerated water larger than the van der Waals attraction? We find affirmative answers to both questions and conclude from our data that (1) in aerated water, bridging nanobubbles are primarily responsible for the long-range hydrophobic attraction, and (2) in deaerated water, nanobubbles are not present and that a different mechanism for the long-range hydrophobic attraction is present. We argue that our deaerated data reveal the bare or pristine hydrophobic attraction unobscured by nanobubbles. The data are consistent with the theoretical mechanism proposed by Bérard et al.,[6] that the attraction occurs approaching a separation-induced spinodal cavitation separation, but prior to the actual onset of cavitation. The idea is that for intermediate separations it is thermodynamically favorable for a vapor cavity to replace the liquid water between the hydrophobic surfaces, but there is a free energy barrier to the formation of such a cavity.[6−8,11,12] As the separation is decreased, the barrier decreases, and it disappears at the spinodal, where it is no longer possible to prevent cavitation from occurring. This is the separation-induced spinodal cavitation referred to in the theory.[6] Approaching such a spinodal, it is possible to show that interactions between solutes become long-ranged and attractive.[30] The interpretation that the present deaerated measurements reveal the pristine hydrophobic attraction unobscured by nanobubbles, and that this may be attributed to the proximity to a spinodal cavitation separation, put into context of previous deaerated force measurements, provide a framework to further advance our understanding of the mechanisms underlying the measured long-range hydrophobic attraction.

Experimental Section

Small glass spheres (Duke Scientific) of radii 3−5 μm, as determined by optical microscopy, were attached to the end of v-shaped cantilevers (Nanoprobe Si_3N_4 NP-S) using a small amount of glue (Shell Epikote) and a tungsten wire as a micromanipulator. The spring constant of cantilevers was measured as 0.15 ± 0.02 N/m,[17] using the fundamental resonance frequency.[31] The atomic force microscope (AFM, Nanoscope IIIa; Digital Instruments, CA) piezo-drive was calibrated interferometricly.[32] The flat surfaces for modification were oxidized silicon wafers mounted on magnetic piezo slides. Both the flat surface and the particle mounted on the cantilever were exposed to (heptafluoroisopropoxy)propylmethlydichlorosilane (Hüls Petrarch Systems) vapor at room temperature and pressure for 30 min before being left to dry for at least 1 day in a laminar flow

(20) Miller, J. D.; Yuehua, H.; Veeramasuneni, S.; Yongqiang, L. *Colloids Surf., A* **1999**, *154*, 137.
(21) Steitz, R.; Gutberlet, T.; Hauss, T.; Klosgen, B.; Krastev, R.; Schemmel, S.; Simonsen, A. C.; Findenberg, G. H. *Langmuir* **2003**, *19*, 2409.
(22) Mahnke, J.; Stearnes, J.; Hayes, R. A.; Fornasiero, D.; Ralston, J. *Phys. Chem. Chem. Phys.* **1999**, *1*, 2993.
(23) Meyer, E. E.; Lin, Q.; Israelachvili, J. N. *Langmuir* **2005**, *21*, 256.
(24) Craig, V. S. J.; Ninham, B. W.; Pashley, R. M. *Langmuir* **1999**, *15*, 1562.
(25) Meagher, L.; Craig, V. S. J. *Langmuir* **1994**, *10*, 2736.
(26) Wood, J.; Sharma, R. *Langmuir* **1995**, *11*, 4797.
(27) Rabinovitch, Ya. I.; Yoon, R.-H. *Colloids Surf., A* **1994**, *93*, 263.
(28) Drummond, C. J.; Georgaklis, G.; Chan, D. Y. C. *Langmuir* **1996**, *12*, 2617.
(29) Welzel, P. B.; Rauwolf, C.; Yudin, O.; Grundke, K. *J. Colloid Interface Sci.* **2002**, *251*, 101.
(30) Attard, P.; Ursenbach, C. P.; Patey, G. N. *Phys. Rev. A* **1992**, *45*, 7621.
(31) Cleveland, J. P.; Manne, S.; Bocek, D.; Hansma, P. K. *Rev. Sci. Instrum.* **1993**, *64*, 403.
(32) Jaschke, M.; Butt, H.-J. *Rev. Sci. Instrum.* **1995**, *66*, 1258.

cabinet. Both fluorosilanated surfaces were then cast in a solution (0.1 wt %) of Teflon AF1600 (Dupont Polymer Products, Wilmington, Delaware) in perfluoro-2-butyltetrahydrofuran (Fluoroinert liquid FC75, 3M, Australia). For the spherical particle, the coating procedure involved dipping the fluorosilanated sphere in the Teflon AF1600 solution. The dipping took place over a few minutes, with slow withdrawal from the coating solution. At the solution concentration and temperature employed, the rheology of the solution, and the surface free energy, ensured that the drainage was such that Teflon AF1600 was retained on the sphere. Care was taken to minimize the amount of Teflon AF1600 coating on the cantilever, especially avoiding polymer bridging across the v-shaped legs. Cantilever spring constant determination was performed after coating. For the flat surface, the coating procedure involved placing a drop of the Teflon AF1600 on the fluorosilanated wafer. The solution wetted the surface. For both the sphere and the flat surface, the first Teflon AF1600 coat was allowed to dry for 2 days before a second coat was applied. Two coats were applied to each sphere, while between 2 and 5 coats were applied to the silicon surfaces, with each coat being allowed at least 2 days to dry before a further coat was applied. We have found that low temperature (no vacuum) slow drying was required to avoid the formation of pinhole defects in the polymer film. In all experiments, the water used was distilled before being passed through a Milli-Q filtration system. No electrolyte was added.

Degassing was performed by freezing water in a sealed 500 mL round-bottomed flask while using a vacuum pump to maintain a pressure of approximately 10 Torr within the flask. Freeze-pumping was continued for 20−45 min before the ice was thawed at the same pressure. At least two, and usually three, freeze−pump−thaw cycles were completed before the degassed water was employed. A tube, which remained sealed during the freeze−pump−thaw process, connected the round-bottomed flask directly to the fluid cell in the AFM; the outlet from the fluid cell was connected to another sealed flask, and the cell was sealed with silicone rubber. Just prior to measurement, the vacuum was removed from the round-bottomed flask containing the degassed liquid (although it remained sealed), and a vacuum was applied to the other flask connected to the output of the fluid cell. The pressure differential between the two flasks then caused the water to be pulled through the cell. The flow of water through the cell was stopped during measurements (to maximize the stability of the force traces) by sealing the tubes in and out of the AFM using plastic clips. This arrangement was designed to minimize the reexposure of degassed water to the air just before and during measurement. Sucking normal (nondegassed) water through in this way was also found to be useful in minimizing the appearance of macroscopic bubbles in the fluid cell (which causes drift of setpoint voltage and disrupts measurement).

This work employed a Nanoscope E (Digital Instruments, Santa Barbara, California) fitted with a K-scanner. Most of the force curves were captured using the continuous approach and force−volume functions (with an absolute trigger set), although it was occasionally necessary to use single approach to improve resolution in the jump-to-contact region.

Results and Discussion

The distributions of the jump-to-contact distances for 55 force curves in normal air equilibrated water and 49 curves in degassed water are shown in Figure 1; the curves represent repeated measurements on a single sphere and surface, first under normal or aerated conditions, then degassed. Each set was captured over a similar time period (roughly 15 min). The irregularity of the data for normal water has previously been taken as evidence for nanobubbles and as indicating variability in their height.[11,13−17] In the data in Figure 1 for aerated water, the flatness of the distribution and the digitization of the levels is a consequence of the relatively few force measurements. There are evidently quantitative and qualitative differences between the aerated and deaerated data in Figure 1. The most likely jump-in distance in aerated water is 56 nm, which is more than 5 times larger than the 11 nm

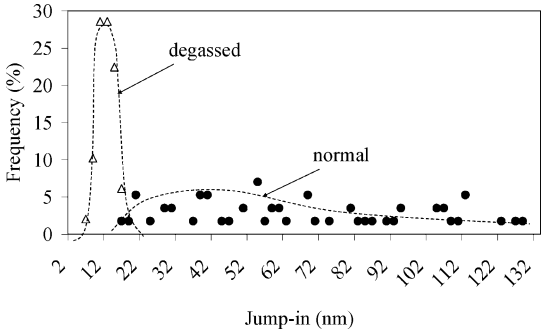

Figure 1. Distribution of jump-to-contact distances for normal (55) and degassed (49) curves. The sphere has radius R = 4.4 μm. The curves are a guide to the eye.

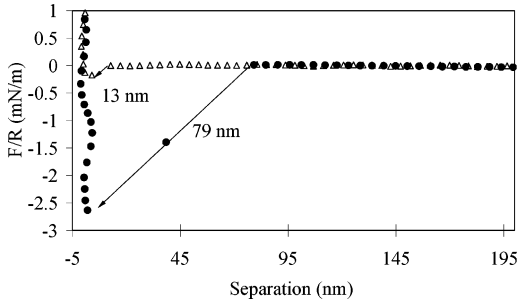

Figure 2. Typical force curve for normal (●) and degassed (△) systems (taken from the data set of Figure 1).

most likely jump-in distance in deaerated water. Also, the distribution of jump-in distances in aerated water is very broad, ranging up to 130 nm. In contrast, in deaerated water, the jump-in distance is quite narrowly distributed about the peak at 11 nm. This narrow distribution indicates that the forces are quite reproducible, as one might expect for a "normal" thermodynamic force, and it strongly suggests that nanobubbles are not present in the deaerated system.[33] However, as is discussed quantitatively below, the force and the jump-in distance in deaerated water are still significantly more than the van der Waals attraction for this system.

Some force curves from the data set from which Figure 1 is taken exhibited a region of exponential repulsion at large separation (probably arising from an electric double-layer effect[13−16]), some showed an attractive curve prior to the jump-to-contact, while others (such as those shown in Figure 2) displayed neither attraction nor repulsion before being abruptly pulled into contact. It can be seen that the jump into contact occurs further out and that the depth of the force immediately after contact is greater in the aerated system than in the deaerated system. A further feature evident in Figure 2 is the noticeable "hook" or soft repulsion in the deaerated data at the end of the jump into contact. This feature has been noted in previous data,[13,16] and it has been quantitatively interpreted as a hydrodynamic drainage repulsion due to the displacement of water by a laterally spreading bridging bubble or cavity.[34] This interpretation of the data for deaerated systems (that a spreading, bridging vapor cavity is present) can in fact be reconciled with that given in the previous paragraph (that no preexisting nanobubbles are present in deaerated systems), as is discussed below.

(33) There is no reason to suppose that if nanobubbles exist in deaerated water, then they would have a more narrow distribution of heights than in aerated water. In any case, thermodynamic arguments indicate that nanobubbles in deaerated water must have a larger radius of curvature than those in aerated water.

(34) Attard, P. *Langmuir* **2000**, *16*, 4455.

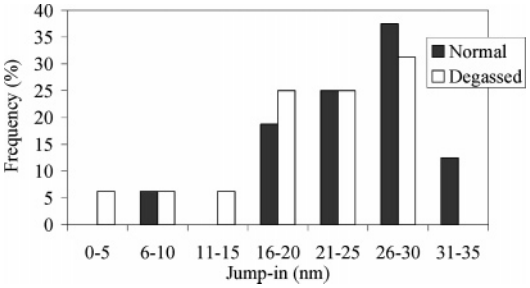

Figure 3. Distribution of jump-to-contact distances for 16 normal and 16 degassed curves ($R = 3.5\ \mu$m).

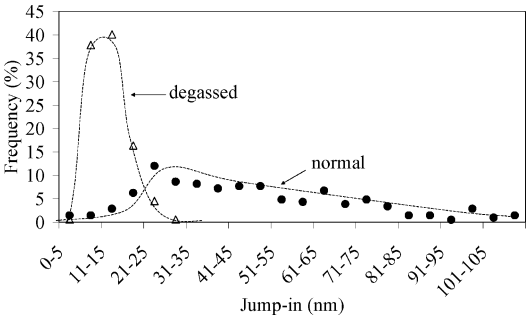

Figure 4. Distribution of jump-to-contact distances for normal (208) and degassed (176) force−volume curves. These measurements were made using the same sphere and surface as in Figure 1. The curves are a guide to the eye.

Figure 3 shows distributions of jump-in distances for 16 normal and 16 degassed force measurements using a sphere 3.5 μm in radius. As compared to the data in Figure 1, the jump distances in Figure 3 are markedly less for the normal case, and slightly greater for the deaerated case. It is evident that in this experiment deaeration obviously has a minor, statistically insignificant effect. Hence, when the jump-to-contact in aerated water was less than ~40 nm, degassing appeared to have little or no effect on the resulting distribution of jump-in distances. A similar conclusion was reached by Mahnke et al.[22] by comparing measurements on different methylated silica surfaces. Our interpretation of the data in Figure 3 is that nanobubbles are not present in either case in this particular experiment. The data suggest that the nucleation of nanobubbles is rather sensitive to the precise experimental conditions and that aeration is a necessary but not a sufficient condition for their presence. The deaerated data in Figure 1 (peak at 11−12 nm and extending to 20 nm) are in broad agreement with the deaearated data in Figure 3 (peak at 16−30 nm, and extending to 30 nm), although they are somewhat smaller. The measured jump-in distances in both the normal and the deaerated data in Figure 3 cannot be accounted for by the van der Waals force.

The force−volume data for the jump-in distance shown in Figure 4 were obtained with the same sphere and surface used as that for the continuous approach curves shown in Figure 1, but on a different day. In Figure 4, the jump-to-contact distances for a large number of force traces (208 normal and 176 degassed) are shown. The force curves were taken at 6.25 μm intervals up to a distance of 100 μm in the scan direction. The colloid probe was then returned to the start location, off-set by −6.25 μm, and the process repeated until the total number of force curves was reached. As in Figure 1, there is a significant reduction in the jump-in distance and in its variability in going to degassed water from aerated water. These force−volume measurements over this very large region rule out the possibility that the data in Figure 1 could have been due to different surface features or inhomogeneities occurring in the two different contact regions used for the aerated and for the deaerated measurements.

There is, however, at least one difference between the repeated contact at a point and the force−volume data. The average jump-to-contact distance for the 55 repeated contact curves in Figure 1 is 65 nm, while the average distance for the 208 force−volume curves in Figure 4 (for the same sphere and surface) is 45 nm. This reduced mean jump-in distance in the force−volume data as compared to the repeated contact data was also present in two other sphere−surface pairs (not shown). These results for aerated water would appear to be consistent with earlier observations that there is an increase in the attraction in going from first contact at a point to subsequent contacts.[35,36] The interpretation of this is that nanobubbles in the contact region grow by rectification at each contact. In the present force−volume plots, the hydrophobic substrate at each contact is pristine even while the hydrophobed probe itself makes repeated contacts. If this interpretation is correct, then the fact that for deaerated water there is no significant difference between the repeated contact data in Figure 1 (mean jump-in distance of 11 nm) and the force−volume data in Figure 4 (mean jump-in distance of 12 nm) implies that nanobubbles are not present in deaerated water.

Figure 5 shows contour images of the jump-in distances measured by the force−volume plot. It can be seen in Figure 5a (aerated water) that the force curves that have large jump-in distances (>60 nm) are clustered at one end of the measurement area. Our interpretation of this is that larger nanobubbles have clustered in this region and that either no nanobubbles or smaller nanobubbles are on the remainder of the surface. If true, this indicates that there is a localized and heterogeneous thermodynamic environment at the surface and that the nanobubbles are not in thermodynamic equilibrium with each other or with the aerated water over the whole of the surface. It has previously been argued that the existence of nanobubbles necessarily implies an absence of thermodynamic equilibrium.[11,12,37] It should be noted that previous AFM images of Teflon AF1600 in air have shown the surface to be smooth and featureless, with a root-mean-square roughness of 0.3 nm and some features up to 3 nm in height.[28] The surfaces were prepared in a manner identical to those reported in our previous work.[17,28] We imaged in air the surfaces employed in the current work and found the surfaces to be very similar to those used in the earlier work. Hence, the marked heterogeneity evident in Figure 5a must be induced by the liquid environment, which supports the nanobubble hypothesis. This interpretation is reinforced by the data in Figure 5b for deaerated water, which is clearly much more homogeneous and uniform (note the scale change between the figures). The most obvious interpretation of the data in Figure 5b is that either nanobubbles are absent, or else if they are present then they form a fairly uniform film or raft on the surface. The latter hypothesis is inconsistent with the widely stated assertion that deaeration decreases the number of nanobubbles on the surface.

Figure 6 shows the distributions of the measured adhesions obtained from the force−volume experiments

(35) Vinogradova, O. I.; Yakubov, G. E.; Butt, H.-J. *J. Chem. Phys.* **2001**, *114*, 8124.
(36) Yakubov, G. E.; Butt, H.-J.; Vinogradova, O. I. *J. Phys. Chem. B* **2000**, *104*, 3407.
(37) Attard, P.; Moody, M. P.; Tyrrell, J. W. G. *Physica A* **2002**, *314*, 696.

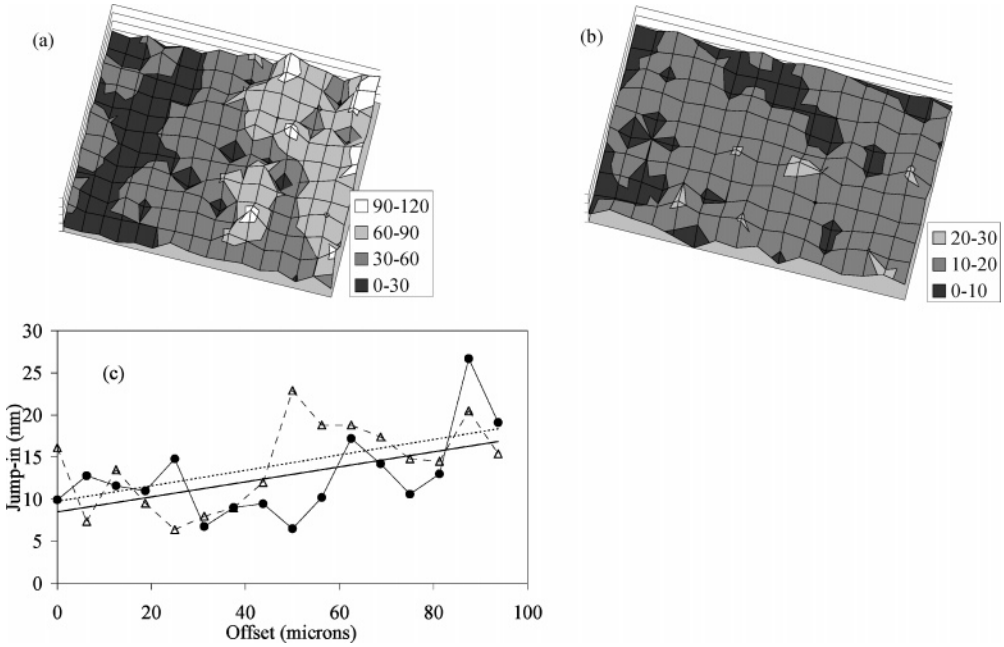

Figure 5. Contour image of jump-in distances over the force−volume region for (a) aerated system (16 × 13 force−volume matrix with a 6.25 μm step size mapping an area of 100 × 84.5 μm) and (b) deaerated system (16 × 11 force−volume matrix with a 6.25 μm step size mapping an area of 100 × 71.5 μm); note change in vertical scale between (a) and (b). This is the same data that are plotted in the distribution in Figure 4. (c) Cross-sectional plot of jump-in distances from two other force−volume regions for a deaerated system (lines are best fits). In all cases, the slow motion of the probe is from left to right.

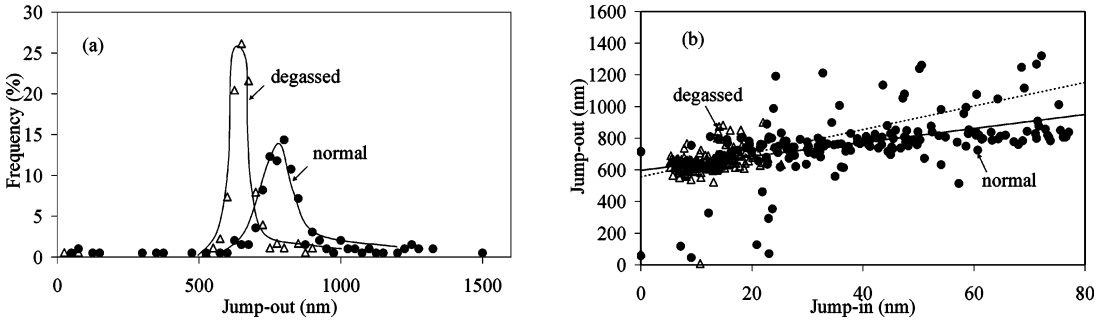

Figure 6. (a) Distribution of adhesion data for normal (208) and degassed (176) force−volume systems. This system is the same as the one shown in Figures 1 and 4 (R = 4.4 μm). (Curves are a guide to the eye.) (b) The jump-in distance versus the jump-out distance for normal and degassed systems, with lines of best fit applied to both systems.

of Figure 4. There is obviously little difference between the degassed (mean jump-out distance approximately 650 nm) and aerated (mean jump-out distance approximately 800 nm). Because a vapor cavity is thermodynamically stable between the hydrophobic surfaces when in contact, and because there is no barrier to its formation in this situation,[7,8,11,12] one expects the adhesion to be due to a capillary vapor bridge in both the aerated and the deaerated systems. The jump-out distance classically expected from a capillary vapor bridge is[34] $-4\pi\gamma R\cos(\theta)/k$, where γ = 72 mN/m is the surface tension of water, k = 0.15 N/m is the spring constant, and θ is the contact angle. Taking $\theta = 120°$ gives a jump-out distance of 13 μm. The classical expression makes a number of approximations that become inaccurate as the size of the particle is decreased. A more accurate expression appropriate for colloidal sized particles[34] that has been tested against exact Eular−Lagrange calculations[34] gives a jump-out distance of 5.1 μm. The discrepancy between the measured and the calculated adhesion is common in AFM measurements and could be due to surface roughness, probe rolling, or kinetic effects. The jump-out distances due to solid−solid adhesion[38] calculated from a Lennard-Jones model of the van der Waals force[39] are of the order of 40−250 nm (using an equilibrium surface spacing of 0.5−0.2 nm).

Figure 6b plots the jump-out distance against the jump-in distance. There is evidently a positive correlation between the two. What is possibly more striking in the figure is the extreme scatter in the jump-out distances. Such scatter is typical of adhesion measurements. Those cases that have very low adhesions also have low jump-in distances (both aerated and deaerated).

Most of the aerated data in Figures 1, 2, 4, and 5 have such a long range that the most reasonable attribution is to bridging nanobubbles. However, the deaerated data in these figures, and both the aerated and the deaerated data in Figure 3, also indicate an attraction much stronger than van der Waals. This is evident from the data in Figure 7 for the R = 3.5 μm sphere. These data were selected as having the shortest jump-in distances of the deaerated data set used in Figure 3. Nevertheless, even these "short-range" data show that the measured attraction is significantly larger than could be expected for the van der Waals interaction for Teflon AF1600 across water, where

(38) Johnson, K. L.; Kendall, K.; Roberts, A. D. *Proc. R. Soc. London, Ser. A* **1971**, *324*, 301.
(39) Attard, P.; Parker, J. L. *Phys. Rev. A* **1992**, *46*, 7959.

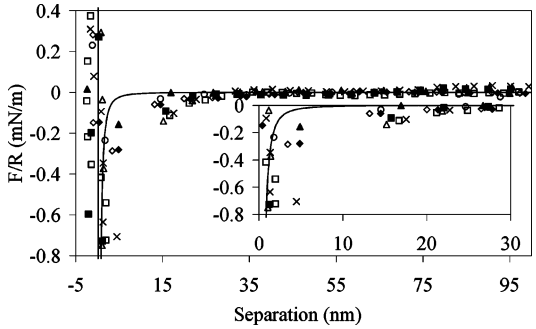

Figure 7. Eight force curves in a degassed system (R = 3.5 μm). The solid curve is the calculated van der Waals interaction (using the nonretarded Hamaker constant for Teflon Af 1600: $A_{FWF}(H_0) = 3.59 \times 10^{-21}$ J).[28] Inset: Magnification of the data around the jump-in.

the Hamaker constant is 3.59×10^{-21} J.[28] Under a pure nonretarded van der Waals interaction, which is the upper limit, jump-to-contact distances would be given by $D_j = (AR/3k)^{1/3}$. This corresponds to a jump-in distance of 3.0 nm for the 3.5 μm sphere used here and in Figure 3, and to a 3.3 nm jump for the 4.4 μm sphere used in the remaining figures. It is evident that the average jump-in distances measured in deaerated water for the larger sphere, 11−12 nm, and 20 nm for the smaller sphere in Figure 3 are 4−7 times greater than could be due to a van der Waals attraction. The data in Figure 7, which have the shortest jump-in distances of the data in Figure 3, jump into contact from about 15 nm, which is about 5 times larger than expected. It is worthwhile also noting that the force−separation curve for Teflon AF1600 surfaces interacting across air is in quantitative agreement with the sole presence of van der Waals interaction.[28] One may conclude from these data and the other deaerated data discussed above that the hydrophobic attraction in deaerated water systems is much stronger than the van der Waals attraction.

In ruling out a van der Waals origin for the attraction, it is necessary to consider the possibility that deformation of the surfaces makes a significant contribution. Using an elastic constant for Teflon AF1600 of $E/(1-\nu^2) = 1.5$ GPa,[40] according to Attard and Parker,[39] the pre-jump stretching of the surface due to the van der Waals force is 0.001 nm. According to JKR theory,[38] the post-jump flattening of the surfaces is 0.16−0.53 nm (using an equilibrium spacing of 0.5−0.2 nm). These calculations are for an infinitely thick film and hence are an upper bound on the actual deformation that occurs. These values rule out deformation playing any role in the forces measured in Figure 7. (This is consistent with the fact that the attractions measured between AF1600 surfaces in air quantitatively agreed with the calculated van der Waals attraction without invoking deformation.[28]) An alternative hypothesis for the large attractions that is related to deformation of soft surfaces is the idea of polymer bridging due to tails or trails extending into the water from the AF1600 surfaces. This possibility seems unlikely given the smooth nature of the surfaces when imaged in air[28] and the fact that water is a poor solvent for this polymer.

In ascertaining the origin of the long-ranged attractions in Figure 7, it is significant that the initial attraction is continuous and extends over many data points. For stiff springs and massive surfaces, nanobubbles cause a discontinuity in the measured force as the attraction begins at the instant of bridging. Indeed, it was these steps or discontinuities in the force that were the original clue to the existence of nanobubbles.[11] For weak springs and colloidal-sized probes, as used in the AFM, the surfaces jump to contact immediately upon bubble bridging because the rate of increase of the force is greater than the spring constant of the cantilever. Such instantaneous jumps have been seen in previous AFM data.[13−17] That this is not the case in the data shown in Figure 7, and that the force of attraction here increases in magnitude smoothly from zero at large separations, indicate that the attractions measured on approach prior to contact in the deaerated system are not due to bridging nanobubbles. For the same reason, they cannot be due to an induced vapor cavity bridging the surfaces.[7−10] The possibility that remains is that it is due to the approach to a separation-induced liquid-spinodal of the type suggested by Bérard et al.[6] In this theory, the bridging vapor cavity has not yet formed, but a long-ranged attraction occurs in the metastable liquid due to the long-ranged correlations that exist in the spinodal region of a bulk fluid.[30] Bérard et al.[6] provided quantitative simulation data to support the theory for a one-component Lennard-Jones liquid, but it should be stressed that the theory applies equally well to the spinodal decomposition of a binary mixture (such as air and water). The adhesion evidence discussed in Figure 6 suggests that a vapor cavity has formed by the time the surfaces are pulled out of contact, from which one can conclude that a spinodal separation for cavitation must exist. The theoretical[6,30] and simulation[6] results indicate that an attraction must occur prior to this separation. These data[6] were obtained for a Lennard-Jones liquid at particular thermodynamic state points and for particular wall−fluid interactions. Hence, those results cannot be applied quantitatively to the present measurements. Nevertheless, the data in Figure 7 are in qualitative agreement with the theory and they indicate that most likely the measured attractions are due to the long-range correlations that exist upon the approach to a separation-induced liquid-spinodal.[6] The present evidence that in the deaerated system the surfaces are free of nanobubbles, and that the reduced variability in the jump-in distance is indicative of a thermodynamic force, is consistent with the interpretation that this separation-induced liquid-spinodal[6] is the origin of the long-ranged attraction between bare or pristine hydrophobic surfaces.

Conclusion

This paper has presented AFM measurements of the long-ranged attraction between hydrophobic Teflon AF1600 surfaces in water. Particular attention has been focused upon the effects of deaeration. In normal or aerated water, it was concluded that the attraction was due to bridging nanobubbles, as first discovered by Parker et al.[11] The present evidence for this was the extremely long jump-in distances, and the highly variable nature of the jump-distances, in agreement with previous measurements.[11,13−19] Despite the variability in the jump-in distance, the large number of measurements allowed the conclusion to be drawn that in a statistical sense the range of the force was significantly reduced upon deaeration. This conclusion is also consistent with earlier deaeration work,[14,22−25] and it supports the nanobubble mechanism.

It was concluded that nanobubbles were not present on the surfaces in deaerated water, which of course is a stronger statement than the alternative conclusion that the nanobubbles were reduced in size or coverage by deaeration. The evidence for our conclusion was that (1) the jump-in distance was reduced, as was the variability in that distance, neither of which would be expected to

(40) Resnick, P. R. *Mater. Res. Soc. Symp. Proc.* **1990**, *167*, 105. The measured Youngs modulus is 0.95−2.15 GPa.

occur if nanobubbles were still present,[33] and (2) prior to the jump into contact there was a measurable attraction that went continuously to zero at larger separation over an extended range. This contrasts with the force due to a bridging nanobubble, which occurs suddenly and discontinuously at the moment of attachment and which immediately causes the surfaces to jump into contact.[11,12] It was concluded that in deaerated water we were measuring the long-ranged attraction between bare or pristine hydrophobic surfaces unobscured by nanobubbles.

It was also concluded that this pristine hydrophobic attraction in deaerated water had the character of a thermodynamic surface force (as opposed to the force due to the physical attachment of nanobubbles). By this is meant that the reduced variability in the jump-in distance means that the force is far more reproducible and that it depends on the nature of the surfaces and the thermodynamic state point of the system (albeit possibly quite sensitively so). The variability that was observed in the jump-in distance in deaerated water may be attributed to the fact that the spring-mounted surfaces are close to a mechanical instability and are easily perturbed by external noise and vibrations, as regularly occurs in measurements of van der Waals jumps, and also of adhesion pull-off forces. The weakest attractions measured here in deaerated water were still at least 4 times greater than the van der Waals forces for this system.

Of the various realistic mechanisms that have been proposed for the hydrophobic attraction in the absence of nanobubbles,[4−10] it was concluded that the present results in deaerated water provided support for the mechanism of Bérard et al.[6] (the approach to a separation-induced liquid-spinodal). The continuous nature of the measured attractions prior to the jump appears to be more consistent with this mechanism than with mechanisms based upon the existence of an already induced vapor bridge,[7−10] which, as for nanobubbles, should cause a sudden and discontinuous jump into contact. While the present data do not directly test electrostatic effects, the fact that the present Teflon AF1600 surfaces possess no charged or ionizable groups, and the fact that there is no added electrolyte in this system, tend to argue against electrostatic fluctuation mechanisms[4,5] in the present system. By this process of elimination, the mechanism of Bérard et al.[6] remains the one that is most consistent with the present results for deaerated water. Further evidence in the present data for this theory is the large adhesions that are measured (pull-off forces), which are consistent with a vapor capillary adhesion. We conclude that such a vapor bridge must have formed either once the surface is in contact, or, more likely, during the final jump into contact. The formation of such an induced vapor cavity indicates in turn that there must exist a spinodal separation beneath which cavitation cannot be prevented, as is a necessary precondition for the theory of Bérard et al.[6] On quite general and formally exact thermodynamic grounds, one can prove that correlations become long-ranged approaching such a spinodal, and that the forces between surfaces must be universally attractive in this regime.[6,30] Hence, one can conclude that the present results are at least qualitatively consistent with the separation-induced liquid-spinodal theory[6] for the pristine hydrophobic attraction. It remains to attempt a quantitative reconciliation of the two.

Acknowledgment. We acknowledge financial support from the Commonwealth Scientific and Industrial Research Organization (H.S.), from the Australian Cooperative Research Centre for Water Quality and Treatment (R.F.C.), and from the Australian Research Council (C.J.D. (Federation Fellowship) and P.A.).

LA0507535